Journal of Molecular Structure 1060 (2014) 280–290

Contents lists available at ScienceDirect

Journal of Molecular Structure

journal homepage: www.elsevier.com/locate/molstruc

Synthesis, Characterization, Thermal and Antimicrobial studies of *N*-substituted Sulfanilamide derivatives

Manu Lahtinen [a], Jyothi Kudva [b,*], Poornima Hegde [b], Krishna Bhat [c], Erkki Kolehmainen [a], Nonappa [d], Venkatesh [e], Damodara Naral [f]

[a] Department of Chemistry, University of Jyväskylä, FI-40014 JY, Finland
[b] Department of Chemistry, St. Joseph Engineering College, Mangalore, India
[c] Department of Chemistry, NITK, Surathkal, Mangalore, India
[d] Aalto University School of Science, Department of Applied Physics, FI-00076 Aalto, Finland
[e] Department of Chemistry and iNANO, Aarhus University Langelandsgade 140, 8000 Aarhus C, Denmark
[f] Department of Chemistry, Canara Engineering College, Mangalore, India

HIGHLIGHTS

- Synthesized four sulfanilamide derivatives.
- Characterized by IR NMR and Mass spectra.
- Single crystal X-ray diffraction study was done.
- The thermal behavior study was done by TGA and DSC methods.
- Antimicrobial activity was studied.

ARTICLE INFO

Article history:
Received 8 August 2013
Received in revised form 17 December 2013
Accepted 18 December 2013
Available online 31 December 2013

Keywords:
Synthesis
Sulfanilamides
Antimicrobial activity
X-ray diffraction
Crystal structure
Thermal analysis

ABSTRACT

Four sulfanilamide derivatives *N*-[4-(phenylsulfamoyl)phenyl]acetamide **(1),** 4-amino-*N*-phenylbenzenesulfonamide **(2),** *N*-[4-(phenylsulfamoyl)phenyl]benzamide **(3)** and *N*-{4-[(3-chlorophenyl)sulfamoyl]phenylbenzamide **(4)** were synthesized and characterized by Infra-Red (IR), Nuclear Magnetic Resonance (NMR) and UV–visible (UV–Vis) spectra. Also Liquid Chromatographic (LCMS) and High Resolution Mass Spectrometric (HRMS) methods were used. Crystal structures of **1–4** were determined by single crystal X-ray diffraction (XRD) and their conformational and hydrogen bond (HB) network properties were examined with survey of the literature data. Compounds **1** and **2** crystallize in the same orthorhombic *Pbca* symmetry with equivalent molecular conformation (tilted V-shape) but showed distinct packing and hydrogen bonding models. Compounds **3** and **4** crystallize in monoclinic and triclinic crystal systems, albeit exhibiting identical molecular conformation (L-shaped). Same donor acceptor pairs both on **3** and **4** result to different kind of HB network. Thermogravimetric (TG) and differential scanning calorimetric (DSC) methods were used to evaluate thermal properties of the substances. All sulfanilamide derivatives have melting points between195–227 °C, initiation of thermal decomposition between 259–271 °C and enthalpies of fusion ΔH^{T}_{fus} = 38.96, 36.60, 46.23 and 44.81 kJ mol^{-1} were determined for **1–4**, respectively. The derivatives were screened for their antibacterial and antifungal activities against various bacterial and fungal strains. It is observed that there is no significant antibacterial activity with the introduction of the benzene ring to CO–NH group or SO_2–NH moiety, and none of the compounds exhibited antifungal activity.

1. Introduction

Sulfonamides represent an important class of medicinally active compounds which are extensively used as antibacterial agents. It interferes with PABA (p-aminobenzoic acid) in the biosynthesis of tetrahydrofolic acid, which is a basic growth factor essential for the metabolic process of bacteria. Many biological activities have been recently reviewed that include endothelia, antagonism, anti-inflammatory, tubular transport inhibition, insulin release and saluretic activity [1]. It is well documented [2–5] that toxicological and pharmacological properties are enhanced when sulfonamides are administered with amide moiety.

* Corresponding author. Tel.: +91 8242232411.
E-mail address: jyothikudva@gmail.com (J. Kudva).

0022-2860/$ - see front matter © 2013 Elsevier B.V. All rights reserved.
http://dx.doi.org/10.1016/j.molstruc.2013.12.063

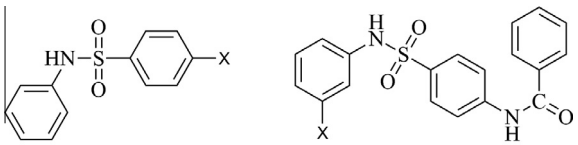

1 : X = $NHCOCH_3$
2 : X = NH_2

3 : X = H
4 : X = Cl

Fig. 1. Molecular structures of compounds **1–4**.

Compounds possessing amide and sulfonamide functional groups have been reported to display a wide range of activities like antibacterial, antifungal [6–9], antiviral [10], anti-tumor [11], anti-malarial [12], anti-HIV [13], anti-ulcer and anti-inflammatory [14], anti-convulsant [15], anti-oxidant [16], anti-coccidiostat [17], hypoglycemic [18], diuretic [19,20], anti-carbonic anhydrase [19,21] antithyroid agents [22] and in the treatment of Alzheimer's disease [23].

Biological and pharmacological properties when coupled with detailed structural studies that reveal great information to design potential drug molecules [24,25]. In this context, we have synthesized some organic compounds bearing amide or sulfonamide moieties (compounds **1–4**, Fig. 1). The identity of these compounds has been characterized by IR, NMR, LCMS, HRMS, UV–visible, TG, DSC and single crystal X-ray diffraction studies. Their antimicrobial activities were evaluated and the results were compared with some of the reported compounds.

2. Experimental

2.1. Physical and chemical measurements

The IR spectra were recorded on a Perkin Elmer FT/IR Spectrum BX in the range 4000–400 cm^{-1} using KBr pellet technique with a spectral resolution 4 cm^{-1}. ^1H and ^{13}C NMR spectra were recorded with Bruker Avance 400 spectrometer in $CDCl_3$ and DMSO-d_6 (400 MHz, ^1H and 100 MHz, ^{13}C). Chemical shifts (δ) were reported in ppm from the internal reference tetramethylsilane (TMS). High resolution mass spectra were measured with Waters Micromass Q-Tof (ESI-HRMS) spectrometer. LCMS measurements were performed in Agilent technologies 1200w series instrument. UV–Visible spectra were obtained in Perkin Elmer Lambda 750. TLC was conducted on 0.25 mm silica gel plates (60F254, Merck). Visualization was made by using ultraviolet light. All the reagents were purchased from commercial sources and used without further purification.

2.1.1. Structure determination by single crystal X-ray diffraction

The intensity data for compounds **1–3** were acquired at −100 ± 1 °C with a Bruker–Nonius Kappa CCD diffractometer equipped with APEXII detector and using graphite monochromatized Mo Kα radiation (λ = 0.71073 Å). The COLLECT [26] software was used for data collection and the data sets were processed with DENZO-SMN [27] and the multi-scan absorption correction (SADABS) [28] was used. For compound **4**, Agilent Supernova (dual source) diffractometer was used to acquire the data at −100 ± 1 °C with multilayer optics monochromatized and micro source generated Cu Kα radiation (λ = 1.54184 Å). Data collection and reduction, as well as analytical numeric absorption correction using a multifaceted crystal model were all made by program Crysalis^{Pro} (v. 1.171.36.24) [29]. All four crystal structures were solved by direct methods using SHELXS [30] and were refined on F^2 using SHELXL-97 [30] both implemented in program Olex^2 (v. 1.2.2) [31]. Hydrogen atoms attached to carbon atoms were calculated to their "idealized" positions as riding atoms, whereas those attached to nitrogen hosts were located in the difference Fourier map. By this, the previously reported zwitterion form [32] plausible for compound **2** was ruled out, as hydrogen atoms attached to the amide and amino groups were possible to locate in the difference Fourier maps. An isotropic extinction parameter was refined in case of compounds **1, 3** and **4**, whereas for **2** its value was negligible and therefore was removed from the final refinement. Isotropic displacement parameters of all hydrogen atoms were fixed 1.2–1.5 times higher than those of the attached non-hydrogen atoms. The programs Mercury (v. 3.0.1) [33] and Olex^2 were used for depicting the crystal structures.

2.1.2. Differential scanning calorimetry

Power compensation-type Perkin–Elmer Pyris Diamond differential scanning calorimeter (DSC) was used to measure DSC heating–cooling scans. DSC scans were made under high purity (999.995%) nitrogen atmosphere (flow rate 50 ml·min^{-1}) using 50 μl aluminum pan sealed by perforated 30 μl aluminum pan. Temperature calibration was carried out with two standards (*n*–decane and In) and energy calibration by an indium standard (Ref. and meas. value 28.45 and 28.47 J·g^{-1}). Each sample was heated at a rate of 10 °C·min^{-1} from −40 °C to about 10–20 °C above the last observed thermal transition (predetermined by TG/DTA), cooled back to −40 °C at a rate of 5 °C·min^{-1}, and then heated similarly for a second time. The sample amounts used on the measurements were about 4–6 mg. The enthalpy of fusion at 298 K was calculated by the equation $\Delta H_{fus}^{298} = \Delta H_{fus} - \Delta S_{fus} - (T_m - 298.15)$, where in $\Delta S_{fus} = \Delta H_{fus}/T_m$.

2.1.3. Thermogravimetry

Thermogravimetric data were recorded with Perkin–Elmer STA 6000 simultaneous thermal analyzer (measuring both thermogravimetric and differential temperature signals; TG/DTA). Each measurement was carried out in an open platinum pan under high purity air (99.999%) atmosphere (flow rate of 45 ml·min^{-1}) by heating a sample from 25 to 700 °C with a heating rate of 10 °C·min^{-1}. Temperature calibration of the instrument was made using melting points of the Perkin–Elmer indium and zinc standards (Ref. and measured values: In 156.6 and 156.5; Zn 419.5 and 419.7 °C, respectively). Weight calibration of the instrument was made at room temperature using amass standard weight (stainless steel) of 50.00 mg. The sample amounts used in the measurements were about 7–8 mg.

2.1.4. Antimicrobial studies

Antibacterial screening of these samples were made against a gram +ve (*S. Aureus*) and a gram –ve (*E. Coli*), in two different concentrations with Ciprofloxacin as reference drug. Testing was done by zone inhibition method in Agar medium. Antifungal studies were done against *Aspergillus niger* and *Candida albicuns* strains with Miconazole as reference drug. Toxicity studies were carried out as per OECD guidelines by giving an oral dose of 2000 mg·kg^{-1}. All compounds were found non-toxic.

2.2. Synthesis of the compounds

2.2.1. Synthesis of N-[4-(phenylsulfamoyl)phenyl]acetamide (*1*) [34,35]

Acetanilide (1.35 g, 0.01 mol) was taken in 10 ml chloroform and cooled to 0 °C. Excess of chlorosulfonic acid (6.7 ml, 0.1 mol) was added in small aliquots maintaining the temperature. The mixture was stirred at RT overnight to complete the reaction as indicated by TLC. Then the reaction mixture was quenched pouring it into crushed ice. Solid separated was filtered, washed with cold

water and dried in nitrogen atmosphere. 4-(acetylamino)benzenesulfonyl chloride was added to 0.91 ml (0.01 mol) aniline in small portions at room temperature at pH 8 by the simultaneous addition of 10% Na_2CO_3. Progress of the reaction was monitored by TLC. After the completion of the reaction, the pH was adjusted to 2.0 by dropwise addition of conc. HCl. The precipitate was collected by filtration, washed with water and dried to afford the compound **1** as white solid. Single crystals suitable for X-ray diffraction studies were obtained from a dilute ethanol/water solution.

Analytical and physical data: Formula: $C_{14}H_{14}N_2O_3S$; Yield: 80–85%; MP: 214–216 °C; LCMS (–ve mode): (M–H) = 289.2 (99.1%), RT – 3.156; HRMS: obtained m/z = 313.0625 (M + Na), cald. = 313.0630.

*2.2.2. Synthesis of 4-amino-N-phenylbenzenesulfonamide (**2**) [36]*

2.9 g (0.01 mol) of compound **1** obtained as per the procedure described above was refluxed with ethanol and conc. HCl till TLC showed completion of the reaction. Reaction mixture was cooled and pH of 9 was maintained using ammonia solution. Separated precipitate was filtered, washed with water and dried. Single crystals of Comp. **2** were grown from water/ethanol solution.

Analytical and physical data: Formula: $C_{12}H_{12}N_2O_2S$; Yield: 85–90%; LCMS (+ve mode): M = 248.9 (98.8%), RT – 2.954; HRMS: obtained m/z = 271.0518 (M + Na), cald. = 271.0517.

*2.2.3. Synthesis of N-[4-(phenylsulfamoyl)phenyl]benzamide (**3**) [9,15]*

To a well-stirred solution of compound **2** (2.48 g, 0.01 mol) in chloroform, benzoyl chloride (1.28 ml, 0.011 mol) in chloroform was added dropwise at 0 °C and stirring was continued in cold condition. After the completion of reaction (monitored by TLC), the reaction mixture was poured into ice cold water. White solid was filtered, washed with acetic acid and sodium bicarbonate solutions, dried and purified by recrystallization. Single crystals suitable for diffraction studies were obtained by slow evaporation from ethanol.

Analytical and physical data: Formula: $C_{19}H_{16}N_2O_3S$; Yield: 70–75%; LCMS (+ve mode): (M + H) = 353.0 (99.5%), RT – 4.349; HRMS: Obtained m/z = 375.0777 (M + Na), cald. = 375.0779.

*2.2.4. Synthesis of N-{4-[(3-chlorophenyl)sulfamoyl]phenylbenzamide (**4**)*

Compound was obtained by the reaction of 4-amino-*N*-(3-chlorophenyl)benzenesulfonamide with benzoyl chloride following the same procedure as mentioned earlier. White crystalline solid was obtained as a final product. Single crystals suitable for diffraction studies were obtained by slow evaporation from ethanol.

Analytical and physical data: Formula: $C_{19}H_{15}ClN_2O_3S$; Yield: 85–90%; LCMS (+ve mode): (M + H) = 387.0(99.5%), RT – 4.868; HRMS: Obtained m/z = 409.0395 (M + Na), cald. = 409.0390.

3. Results and discussion

3.1. IR spectroscopy

The experimental IR frequencies for the compounds are also given in Table 1 (for sample spectra see Supplementary material Fig. S1). The spectra of synthesized compounds contains some characteristic bands of the stretching vibrations of the N—H, C═O and SO_2 groups. The N—H stretching vibration of secondary amines groups of some aryl sulfonamides occurs in the region 3300–3200 cm^{-1} [37]. The bands at 3245 – 3145 cm^{-1} are assigned to the N—H stretching mode of —SO_2NH—. The bands at 3380 – 3291 cm^{-1} are assigned to the N—H stretching mode of —CONH—. This N—H bond appears to be somewhat higher than N—H stretching mode of —SO_2NH—, because —CONH— is more electron withdrawing group. The amides and sulfonamides are strongly associated with hydrogen bonds. The splitting wave number difference in the N—H vibrational bands shows the presence of intermolecular hydrogen bonding by the NH group. The SO_2 asymmetric and symmetric stretching vibrations appeared in the range 1327–1317 cm^{-1} and 1157–1152 cm^{-1} respectively. Compounds showed a strong band in the range 1673–1662 cm^{-1} which is assigned to C═O stretching vibration.

3.2. NMR spectroscopy

The experimental ^1H and ^{13}C NMR chemical shifts for the compounds in DMSO-d_6 are given in Table 2 and Table 3, and the numbering of atoms in Fig. 2 (for sample spectra see Supplementary material Fig. S2). The aromatic carbon signals are assigned between 150.86 and 113.14 ppm and the shift of the carbonyl carbon is between 169 and 166 ppm. Aromatic proton peaks were observed at about 7.94–6.39 ppm. The N—H proton signals appear in the range 10.57 ppm to 10.21 ppm for **3** and **4**, whereas for **1** they appear at 9.52 ppm and 9.26 ppm. But for compound **2**, one N—H proton signal appears at 8.99 ppm and other two N—H proton signals merged with aromatic proton signals i.e. at 6.99 to 6.91 ppm. Again the difference in the chemical shift values of N—H proton signal shows the presence of intermolecular hydrogen bonding by the NH group.

3.3. UV–Visible spectroscopy

The spectral band (λ_{max}) values from the recorded UV–Vis spectra are given in Table 1 and the spectra in Fig. 3. UV–Vis spectra of the synthesized compounds were recorded using ethanol as solvent. The characteristic UV bands with λ_{max} around 230 and 270 were indicative of the presence of benzene chromophore and sulfonamide moiety.

Table 1
IR and UV–Vis spectral data.

Comp.	IR data (Å)						UV
	NH (str)	SO_2 (str)	SO_2 (bend)	C═O(str) (amide I)	NH deform (amide II)	NH (out-of-plane)	λ_{max} (nm)
1	3291.72(m) 3240.12(m)	1316.57(s)assy 1153.81(s)sym	542.39(m)	1673.39(s)	1538.53(s)	730.38(w)	204, 223, 263
2	3421.84(m) 3351.21(m) 3244.57(m)	1318.65(s)assy 1151.56(s)sym	545.99(m)		1639.98(s) (scissoring)		202, 232, 268
3	3355.78(m) 3161.19(m)	1321.58(s)assy 1152.57(s)sym	555.52(w)	1663.01(s)	1537.14(s)	719.49(w)	205, 230, 279
4	3380.17(m) 3145.49(m)	1326.45(s)assy 1156.99(s)sym	546.91(w)	1661.32(s)	1529.49(s)	726.04(w)	204, 230, 277

Table 2
^{1}H NMR chemical shift (ppm) values.

Protons	Comp.			
	1	**2**	**3**	**4**
H_a	9.52	8.99	10.57	10.57
H_b	9.26		10.21	10.48
H_2, H_6	7.55–7.49	7.32	7.94–7.92	7.96–7.91
H_3, H_5	7.55–7.49	6.99–6.91	7.94–7.92	7.96–7.91
H_8	7.03–6.87	6.39	7.10	7.08–7.06
H_9	7.03–6.87	6.99–6.91	7.23	
H_{10}	7.03–6.87	6.81	7.01	7.12
H_{11}	7.03–6.87	6.99–6.91	7.23	7.26
H_{12}	7.03–6.87	6.39	7.10	7.08–7.06
H_{14}, H_{18}	1.98(CH_3)		7.74	7.76
H_{15}, H_{17}	1.98(CH_3)		7.62–7.51	7.62–7.58
H_{16}	1.98(CH_3)		7.62–7.51	7.62–7.58

Table 3
^{13}C NMR chemical shift (ppm) values.

Carbons	Comp.			
	1	**2**	**3**	**4**
C_1	133.11	126.34	134.42	134.37
C_2	127.64	128.46	127.75	127.75
C_3	118.56	113.14	119.90	119.97
C_4	142.47	150.86	143.05	143.31
C_5	118.56	113.14	119.90	119.97
C_6	127.64	128.46	127.75	127.75
C_7	137.17	137.63	137.79	139.40
C_8	120.38	120.03	120.01	118.92
C_9	128.55	128.63	129.09	133.2
C_{10}	124.3	123.39	123.94	123.56
C_{11}	128.55	128.63	129.09	130.87
C_{12}	120.38	120.03	120.01	117.86
C_{13}			133.69	134.37
C_{14}			127.74	127.75
C_{15}			128.43	128.40
C_{16}			131.92	131.92
C_{17}			128.43	128.40
C_{18}			127.74	127.75
C=O	169.22		166.07	166.06
R	22.9 (CH_3)			

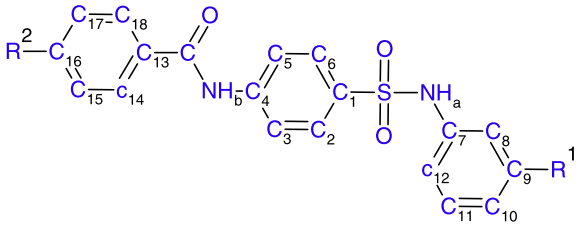

Fig. 2. Atom numbering of the core unit in case of NMR data.

3.4. Single crystal X-ray diffraction analysis

Crystal structures of all four sulfanilamide derivatives were determined by single-crystal X-ray diffraction (XRD). The crystallographic parameters, selected bond distances and angles, dihedral angles and hydrogen bonding geometries are shown in Tables 4–6. In order to properly compare the molecular conformations of the examined compounds, the same numbering scheme and handedness were used on each compound (Fig. 4). General trends on the various conformations were further surveyed by performing geometry related searches using CCDC ConQuest (v. 1.14) and Cambridge crystallographic database (CSD; v. 5.33 Aug. 2012) [38]. Six dihedral angles $\theta_{1\text{-}6}$ were selected for the survey (Table 4 and Fig. 4), of which for comparability purposes the first four were set to be analogous to that of used by Perlovich et al. [39a,39b] and Parkin et al. [40] in their comparative conformation analyses on number of sulfonamides. Based on our atomic numbering scheme, dihedral angles $\theta_{1\text{-}6}$ were defined as follows: for sulfamoyl group region θ_1(N4—S1—C11—C12), θ_2(C11—S1—N4—C5) and θ_3(S1—N4—C5—C6); θ_4 as acute angle between the least- squared planes set through the phenyl groups Ph1 (C5—C6—C7—C8—C9—C10) and Ph2 (C11—C12—C13—C14 —C15—C16); and for amide region θ_5(C18—N17—C14—C13) and θ_6(N17—C18—C20—C21); and notation analogy with references [39–40] is as follows: $\theta_1 = \angle\tau_1$, $\theta_2 = \angle\tau_2$, $\theta_3 = \angle\tau_3$, and $\theta_4 = \angle$Ph1—Ph2).

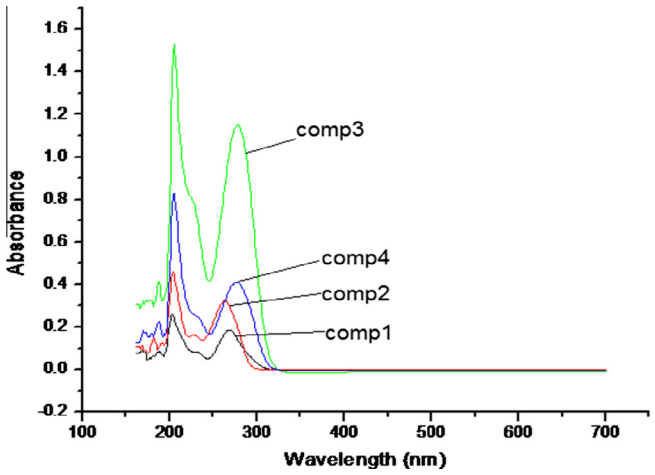

Fig. 3. UV–Vis absorption spectra of compounds **1**–**4**.

The examined sulfanilamide derivatives **1**–**4** crystallize without solvent molecules, in orthorhombic *Pbca* (**1** and **2**), monoclinic $P2_1/c$ (**3**), and triclinic *P*-1 (**4**) space groups having a single crystallographically independent molecule in their asymmetric units (Table 4, Fig. 4). Characteristic geometries, typical bond distances and angles were determined for the main functional groups (e.g. sulfamoyl, acetamide, phenyl), and the structure models were free of any disordered atom sites. Due to rigid geometry of a sulfanilamide core unit, its conformation turned out to be practically the same in all cases. Minor differences can generally be observed in tilting of the phenyl (Ph1) group in relation to the sulfamoyl and phenyl (Ph2) groups, as well as tilting of benzamide phenyl (Ph3) group in relation to the amide group (Table 5 and Fig. 5). As can be seen in Fig. 5, the tilting of Ph1 group on **1** and **2** is equivalent but clearly different to that found on **3** and **4**, where in more perpendicular positions of phenyl group in relation to the sulfanilamide unit is evident. Moreover the conformations of **3** and **4** differ from each other by tilting of Ph3 phenyl group that is somewhat closer to a planar orientation on **3**. Structural similarity search from the CSD revealed number of sulfonamide structures having analogous conformational states for **1** and **2**, like in N^1-2-chlorophenylsulfanilamide [CSD entry: CLPSAM] [41], 4-Amino-N-(5-chloro-2-methylphenyl)benzenesulfonamide [HUNXUK] [42], N-(4′-nitrophenylsulfonyl)-4-iodoaniline [MEZGON] [43], N^1-phenylsulfanilamide [CEYYAG] [32], and many of those reported in extensive sulfonamide studies of Perlovich et al. [39a–d]. Similar molecular conformations with **3** and **4** can be found in N-(4-((4-methylphenyl)-sulfamoyl)-phenyl)acetamide [DUTDEC] [44], 3-(((4-acetamidophenyl)-sulfonyl)amino)benzoic acid [QAJMOF] [45], 4-aminoacetyl-N-p-nitrophenylsulfanilamide [SAZJEI] [46] and in our previously reported N-(4-((3-methylphenyl)-sulfamoyl)

Table 4
Crystallographic data of compounds **1**–**4**.

Comp.	**1**	**2**	**3**	**4**	Ref. [47]
Empirical formula	$C_{14}H_{14}O_3SN_2$	$C_{12}H_{12}O_2SN_2$	$C_{19}H_{16}O_3SN_2$	$C_{19}H_{15}ClO_3S\ N_2$	$C_{20}H_{18}N_2O_3S$
Formula weight	290.33	248.30	352.40	386.84	366.42
Temperature/°C	−100(1)	−100(1)	−100(1)	−100(1)	−100(1)
Crystal system	Orthorhombic	Orthorhombic	Monoclinic	Triclinic	Triclinic
Space group	Pbca	Pbca	$P2_1/c$	$P-1$	$P-1$
a (Å)	12.5848(7)	5.9982(3)	8.9091(9)	8.4815(9)	8.5344 (2)
b (Å)	9.7577(3)	15.6227(8)	8.4554(7)	8.8842(9)	8.8477 (3)
c (Å)	23.1777(10)	24.4198(11)	23.110(2)	12.5632(16)	12.4383 (4)
α (°)	90.00	90.00	90.00	76.741(10)	77.924 (2)
β (°)	90.00	90.00	93.035(9)	75.174(10)	75.382 (2)
γ (°)	90.00	90.00	90.00	87.247(8)	86.537 (2)
Volume (Å^3)	2846.2(2)	2288.33(19)	1738.4(3)	890.69(17)	888.67 (5)
Z	8	8	4	2	2
ρ_{calc} (mg/mm^3)	1.355	1.441	1.346	1.442	1.369
m (mm^{-1})	0.236	0.273	0.206	3.185	0.210
F(000)	1216	1040	736	400	384
Crystal size (mm^3)	0.35 × 0.28 × 0.25	0.31 × 0.26 × 0.14	0.26 × 0.2 × 0.12	0.19 × 0.16 × 0.11	
2Θ range for data collection	5.56–52°	5.22–51.98°	5.14–58.68°	7.48–136.94°[a]	
Reflections collected	11962	5686	15798	5064	
Independent reflections	2796 $R_{(int)}$ = 0.0411	2249 $R_{(int)}$ = 0.0327	4208 $R_{(int)}$ = 0.0402	3227 $R_{(int)}$ = 0.0293	
Data/restraints/parameters	2796/2/191	2249/15/166	4208/2/235	3227/2/244	
Goodness-of-fit on F^2	1.034	1.043	1.046	1.062	
Final R indexes [$I \geqslant 2\sigma$ (I)]	R_1 = 0.0456, wR_2 = 0.1041	R_1 = 0.0483, wR_2 = 0.0953	R_1 = 0.0495, wR_2 = 0.0968	R_1 = 0.0396, wR_2 = 0.1008	
Final R indexes [all data]	R_1 = 0.0757, wR_2 = 0.1256	R_1 = 0.0803, wR_2 = 0.1167	R_1 = 0.0852, wR_2 = 0.1136	R_1 = 0.0470, wR_2 = 0.1093	
Largest diff. peak/hole (e Å^{-3})	0.23/−0.30	0.20/−0.29	0.26/−0.30	0.25/−0.40	

[a] Cu – radiation.

Table 5
Selected bond distances (Å) and angles (°) of **1**–**4** with dihedral angles θ_{1-6}.

Comp.	**1**	**2**	**3**	**4**	Ref. [47]	Mean angle	No. of entries[a]
Distances							
S1—O2	1.4235(18)	1.4325(19)	1.4360(14)	1.4375(14)	1.4399(13)		
S1—O3	1.4299(17)	1.431(2)	1.4232(14)	1.4296(15)	1.4328(14)		
S1—N4	1.643(2)	1.631(2)	1.6219(18)	1.6314(18)	1.6281(17)		
S1—C11	1.748(3)	1.749(3)	1.7590(19)	1.7607(19)	1.7642(19)		
N4—C5	1.439(3)	1.439(3)	1.417(3)	1.424(3)	1.428(3)		
N17—C18	1.346(3)		1.352(2)	1.360(3)	1.360(2)		
C18—O19	1.218(3)		1.220(2)	1.225(2)	1.231(2)		
Angles							
O3—S1—O2	119.04(11)	119.04(13)	119.27(9)	119.02(9)	118.60(8)		
N4—S1—C11	106.34(11)	108.27(12)	107.88(9)	107.27(9)	107.99(8)		
C5—N4—S1	117.38(15)	119.10(19)	125.79(15)	124.09(15)	124.74(13)		
N17—C18—O19	122.2(2)		121.98(19)	122.88(18)	122.61(17)		
Dihedral angles							
θ_1(N4—S1—C11—C12)	−82.4(2)	−77.7(2)	−74.35(18)	−73.41(18)	−69.07(17)	86.07	538
θ_2(C11—S1—N4—C5)	−59.8(2)	−57.6(3)	−62.69(18)	−62.66(18)	−60.65(17)	63.29	538
θ_3(S1—N4—C5—C6)	−77.1(3)	−80.0(3)	−18.8(3)	−28.6(3)	−24.1(3)	112.30	538
θ_4(Ph1···Ph2)	41.36(10)	53.49(9)	89.03(8)	95.44(7)	93.84(6)	68.10	538
θ_5(C18—N17—C14—C13)	30.1(4)		12.3(3)	19.2(3)	21.41(19)	15.03[b]	81
θ_5(C18—N17—C14—C13)[c]						30.20[b]	3312
θ_6(N17—C18—C20—C21)			−161.9(2)	−144.6(2)	−150.49(18)	28.62[b]	10
θ_6(N17—C18—C20—C21)[c]						28.19[b]	1522

[a] Searches were limited to structures having 3D coordinates determined and R-value ⩽ 10%.
[b] Two population exist on angular ranges of ∼0–50° and 140–180° depending on the bearing of the carbonyl group in relation to the attached phenyl group (Ph2) and whether above plane or below plane torsion angle was retrieved by the ConQuest. To have comparable value, absolute angles were reduced to be independent of carbonyl direction by setting angle range to vary from 0 to 90°.
[c] Data retrieved with a fragment not having SO_2NH group attached to the *para*-position of Ph2 group.

phenyl)benzamide [YAGBOZ] [47], to mention few. Overlays of **1**–**4** with selected sulfonamide conformations can be seen in Fig. 5 (see also Supplementary material Fig. S4).

The conformational modes were inspected further using above described dihedral angles θ_1 - θ_6, of which statistical variations retrieved from the CSD are shown in Supplementary Fig. S5. Based on the survey dihedral angle θ_1, describing the orientation of the NH group in relation to a Ph2 group, varies generally about from 45° to 135° with mean average of 86.7°, thereby indicating the almost perpendicular to be the most preferable conformational state for phenyl group Ph1. In contrast to θ_1, angular variation for dihedral angle θ_2 is clearly less and "rotation angle" (S1—N4 bond as rotation axis) of about 60° (mean angle 63.29°) between the Ph1 and Ph2 phenyl groups is strongly favored. Broader range of variation occurs in dihedral angle θ_3, describing the rotational angle of Ph1 group in relation to the NH group, as it varies more or less equally across a semicircle; dihedral angles above ∼75° being somewhat more favored (mean 112.3°) among others. It should also be noted that on the amidated sulfonamides, the lower end of the angular range is favored instead; as in the case of **3**, **4**, [SAZJEI] [46] and

Table 6
Hydrogen bonding geometry for compounds **1**–**4**.

D–H···A	D–H	H···A	D···A	D–H···A	No. of entries
1					
N4–H4···O3 (i)	0.87 (2)	2.13 (2)	2.983 (3)	169 (3)	
N17–H17···O19 (ii)	0.89 (2)	1.96 (2)	2.847 (3)	174 (2)	
2					
N4–H4···N17 (iii)	0.83(2)	2.46(2)	3.202(4)	151(3)	
N17–H17A···O2 (iv)	0.87(2)	2.47(3)	3.104(4)	131(3)	
N17–H17B···O3 (v)	0.87(2)	2.30(2)	3.089(4)	151(3)	
3					
N4–H4···O19 (vi)	0.85 (2)	2.03 (2)	2.846 (2)	162 (2)	
N17–H17···O2 (vii)	0.86 (2)	2.18 (2)	3.002 (2)	159 (2)	
4					
N4–H4···O19 (viii)	0.86 (2)	2.01 (2)	2.824 (2)	158 (2)	
N17–H17···O2 (ix)	0.87 (2)	2.30 (2)	3.017 (2)	139 (2)	
Ref. [47]					
N4–H4···O19[a]	0.86(2)	1.99(2)	2.813(2)	160(2)	
N17–H17···O2[a]	0.84(2)	2.38(2)	3.062(2)	140(2)	
Survey					
N–H···X (O, N)[b]		2.13	2.93	161	328
N–H···X (O, N)[c1]		2.10	2.95	168	79
N–H···X (O, N)[c2]		2.08	2.90	161	2329

Symmetry codes: (i) $-x+1/2, y+1/2, z$; (ii) $-x-1/2, y-1/2, z$; (iii) $-x-1/2, y+1/2, z$; (iv) $-x-1/2, y-1/2, z$; (v) $-x+1/2, y-1/2, z$; (vi) $-x+1, -y+2, -z$; (vii) $x, y-1, z$; (viii) $-x-1, -y, -z$; (ix) $x-1, y, z$.

[a] The labeling used here is different to that of found in Ref. [47].

[b] Data retrieval with SO_2NH donor. Amide fragment with[c1] and without[c2] SO_2NH attached to the *para*-position of Ph2 group.

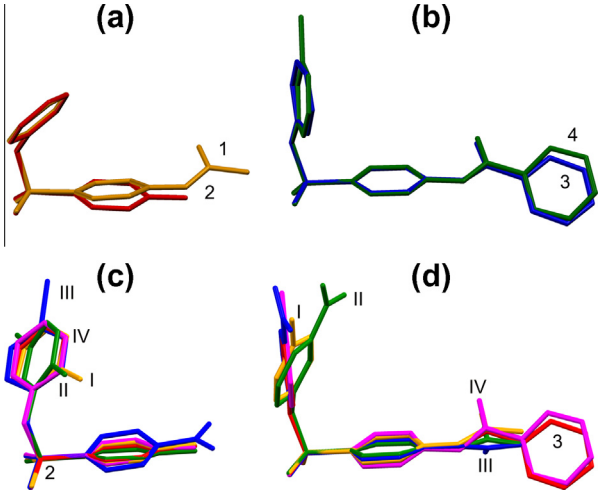

Fig. 5. Molecular conformations of **1**–**4** shown with few comparable structures found in the CSD. (a) **1** and **2**; (b) **3** and **4**; (c) **2** (red line) [$\theta_4 = 53.49°$] with **I** [CLPSAM; yellow, $\theta_4 = 49.65°$] [41], **II** [HUNXUK; green, $\theta_4 = 67.61°$] [42], **III** [MEZGON; blue, $\theta_4 = 31.37°$] [43] and **IV** [CEYYAG; pink, $\theta_4 = 50.67°$] [32]; and (d) **3** (red line) [89.03°] with **I** [DUTDEC; yellow, $\theta_4 = 67.03°$] [44], **II** [QAJMOF; green, $\theta_4 = 63.21°$] [45], **III** [SAZJEI; blue, $\theta_4 = 88.89°$] [46] and **IV** [YAGBOZ; pink, 86.17°] [47]. θ_4 = acute angle between the planes running through Ph1 and Ph2 phenyl rings. (For interpretation of the references to color in this figure legend, the reader is referred to the web version of this article.)

[YAGBOZ] [47] with θ_3 varying merely from ~15° to 24°. The distribution of θ_4 angles show an increasing trend towards higher angles (varying about from 30° to 90°) and having average of 68.10° among ~530 sulfonamide entries found in the database (Table 5). Further analysis of the distribution reveals local "maximum" that exist in the angular range (40–50°) representing the tilted Ph1 conformations found in **1** ($\theta_4 = 41.4°$), **2** ($\theta_4 = 53.5°$), and for instance in N-(4-chlorophenyl)-benzenesulfonamide ($\theta_4 = 54.4°$) [39b]. The second maximum is located around the mean value range ~65–70° to which structural examples are for instance 4-amino-N-(4-methoxyphenyl)-benzenesulfonamide ($\theta_4 = 60.7°$) and N-phenyl-benzenesulfonamide ($\theta_4 = 64.4°$) [39b]. The third and more populated maximum is located closer to angular range 80–90°, that includes many of the amidated sulfonamides such as **3**,

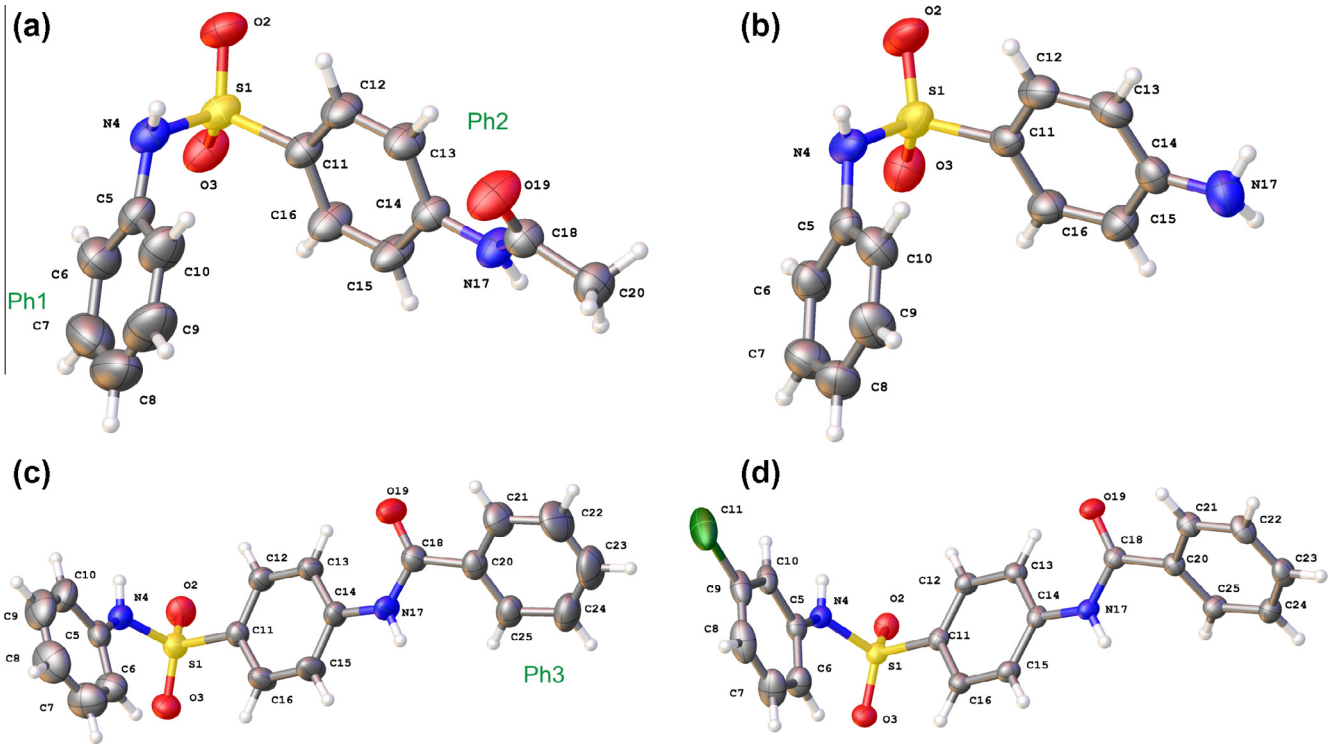

Fig. 4. Asymmetric units of (a) **1**, (b) **2**, (c) **3** and (d) **4** along with the atomic numbering. Thermal displacement ellipsoids are shown at 50% probability.

4 and those reported in the references [47–50]. As expected the dihedral angles θ_5 and θ_6 show clearly the low mobility of the amide group, as both angles vary within narrow range of 0 to about 30° (either below or above the NCO plane) among over 3300 reported amide containing structures found in the CSD. It also appears that the angular range of θ_5 is somewhat affected by the fact whether the sulfamoyl (SO_2NH) group is located in the *para*-position of phenyl Ph2 group or not, as closer to planar orientation (~15°) is preferred when the *para*-position is occupied. However, no significant change can be observed in θ_6 with or without sulfamoyl group, as the mean angle is about 28°in both cases.

Despite of conformational similarities prevailing among various sulfonamides, the molecular packing schemes can differ considerably depending on the available palette of intermolecular interactions present in the crystal lattice (e.g. hydrogen and halogen bonding; vander Waals, π–π and CH–π interactions). As described above, **1** and **2** exhibit practically the same molecular conformation (tilted V-shape), crystallize in orthorhombic *Pbca* space group, have same number of hydrogen bonding (HB) donors, and have relatively similar unit cell dimensions but due to different proton donor–acceptor groups the molecular packing and intermolecular interaction networks are clearly dissimilar. In case of **1**, hydrogen bonding (HB) network is formed from sulfonamide and amide donors (N4—H4 and N17—H17) to the same functional groups on nearby molecules acting as acceptors (O3 and O19), thus HBs exist between amide–amide and sulfonamide–sulfonamide groups with D···A distances varying from ~2.8 to 3.0 Å (Fig. 6 and Table 6). The presented HB geometry can also be categorized using so-called graph set notations described by Etter [51]. With given notations

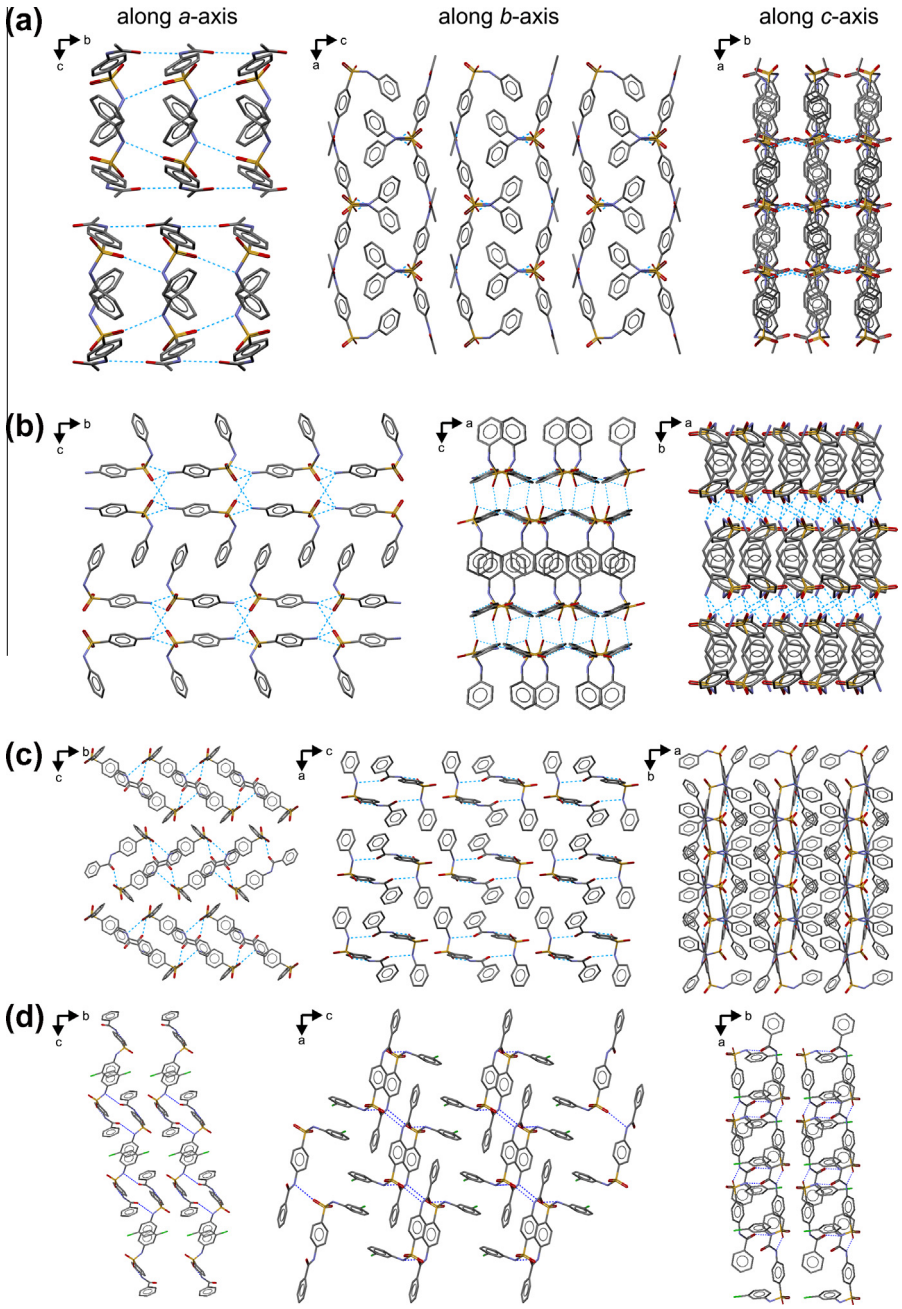

Fig. 6. Depictions of HB networks (dashed blue lines) viewed along crystallographic *a*-, *b*- and *c*-axes, (a) **1**, (b) **2**, (c) **3** and (d) **4**. Hydrogen atoms are removed for clarity. (For interpretation of the references to color in this figure legend, the reader is referred to the web version of this article.)

parallel C(4) type of HB chains (···H—N—C—O··· and ···H—N—S—O··· mediated; see [52]) are running orthogonally through layers of molecules packed parallel to *ac*-plane. Combination of basic HB geometries form a larger second level $R_4^4(26)$ type HB rings mediated by four molecules. The molecules are packed so that phenyl groups Ph1 are showing face-to-edge like arrangement but the π–π contact distance is rather long (~5.7 Å) indicating only weak interaction between these phenyl groups. In compound **2**, more complex HB network is formed via amino (N17—H17a and N17—H17b) donors and sulfamoyl group acceptors (O2 and O3), as well as from sulfonamide donor (N4—H4) to amino (N17) acceptor. By this, parallel HB chains of $C_2^2(6)$ type (···H—N—H···O—S—O···) are running through *a*-axis (D···A = ~3.1 Å), whereas zigzag HB chains of C(8) type (mediated by 4-aminophenyl-sulfamoyl groups) goes along *b*-axis. Also second level $R_4^4(22)$ and $R_2^2(6)$ HB rings exist in the structure as combination of the basic HB units. Moreover, weak π–π interactions exists between adjacent phenyl groups having face-to face and face-to-edge distances of 3.838(2) and 5.318(2) Å, respectively. As a result layer like molecular packing is formed in the crystal lattice wherein HB network and aromatic phenyl group regions alternate. On compound **3**, the L-shaped molecules are packed alongside each other in antiparallel manner. Amide and sulfamoyl groups act both as HB donors and acceptors forming C(8) type HB chain parallel to *b*-axis. These HBs participate to two larger almost orthogonally linked two- and four-molecule membered HB rings with $R_2^2(20)$ and $R_4^4(16)$ geometry types in which amide-sulfonamide donor–acceptor pairs alternate. In addition, face-to-edge (5.309(1) Å) and twisted parallel type of π–π interactions (4.771(1) Å via the phenyl groups are also visible in the crystal structure (Fig. 6c). Compound **4** as well as our previously published sulfanilamide derivative [47], having N-substituted chlorophenyl and methylphenyl groups respectively, follow resembling packing modes than on **3** (Figs. 6 and S6 for [47]), despite of crystallizing in a lower triclinic symmetry. The same donor–acceptor groups form HB network showing again orthogonally linked $R_2^2(20)$ and $R_4^4(16)$ type HB geometries with analogous D···A distances of about 2.8–3.0 Å. Analogous π–π interactions can be identified in the structures in form of face-to-face and several face-to-edge contacts with an average ring centroid distances of 3.6 and 4.7–5.0 Å, respectively. It is also noticeable that the chlorophenyl in compound **4** is not participating to the hydrogen bonding but instead forms face-to-face π–π contacts that is geometrically identical to that of found in methylphenyl substituted sulfanilamide. In a broader view majority of HB geometries observed on compounds **1**–**4** are frequently found in other sulfonamides, of which the C(8), $C_2^2(6)$ and $R_4^4(22)$ type HB geometries (on **2**–**4)** are one of the most common ones [39a–d]. The observed $R_2^2(20)$ and $R_4^4(16)$ type HB geometries seem to be somewhat more common for amidated sulfonamides, as in addition to the examined ones resembling HB geometries were also found in amidated sulfonamides, such as DUTDEC [44], QAJMOF [45] and SAZJEI [46]. Finally, brief literature search on HB distances using various donor–acceptor combinations [N—H···X (O, N)] revealed typical HB distances to have statistical mean values of 2.90–2.95 Å, which are also consistent with now reported parameters.

3.5. Thermal analysis

Thermoanalytical results obtained by differential scanning calorimetric (DSC) and simultaneous thermogravimetric and differential temperature (TG/DTA) analyzers are summarized in Tables 7

Table 7
Thermodynamic characteristic of **1**–**4** with the literature data.

	1	**2**	**3**	**4**	**R1** [39b]	**R2** [39b]	**R3** [39b]	**R4** [53]	**R5** [53]	**R6** [53]
T_m (°C)	211.5	195.2	227.9	225.2	188	204	175	259	236	244
T_m (K)	484.6	468.3	501.1	498.4	461.0	477.6	448.4	532.2	519.2	517.2
ΔH_{fus}^{T} [a]	38.96	36.60	46.23	44.81	39.6	45.6	32.4	40.7	36.4	45.2
ΔH_{fus}^{298} [a]	23.97	23.29	27.51	26.81	25.6	28.5	21.5	22.8	20.9	26.1
ΔS_{fus}^{T} [b]	80.38	78.16	92.27	89.91	85.9	95.5	72.3	76.6	70.1	87.4

$\Delta S_{fus}^{T} = \Delta H_{fus}^{T}/T_3$; R1 = 4-amino-N-(2-bromo-4-nitro-phenyl)-benzene-sulfonamide; R2 = 4-amino-N-(3-chloro-4-methylphenyl)-benzene-sulfon-amide; R3 = 4-amino-N-(3-methoxy-pyrazinyl)-benzene-sulfonamide; R4 = sulfadiazine; R5 = sulfamerazine; and R6 = sulfisomidine. kcal values reported in Ref. [53] were changes to kJ mol^{-1} and not reported ΔH_{fus}^{298} values were calculated.

[a] ΔH = kJ mol^{-1}.

[b] ΔS = J mol^{-1} K^{-1}.

Table 8
Thermoanalytical results of **1**–**4**.

Step	Decomp. onset T $T_{dec.}$ (°C)	T range (°C)	Weight loss/step (%)	Weight loss, overall (%)	DTG_{max} (°C)	DTA_{max} (°C)
1						
1	271	265–303	6.07		283	289 (exo)
2		303–423	52.95		332	335 (endo)
3		423–679	40.94	99.96	567	527 (exo)
2						
1	257	238–306	22.85		279	279 (endo)
2		306–352	28.11		322	322 (endo)
3		352–676	48.87	99.83	542	496 (exo)
3						
1	261	254–309	5.97		277	275 (exo)
2		309–367	47.39		335	337 (endo)
3		367–678	45.93	99.29	585	596 (exo)
4						
1	261	249–314	24.41		294	266 (exo)
2		314–365	32.49		328	329 (endo)
3		365–685	42.96	99.86	576	572 (exo)

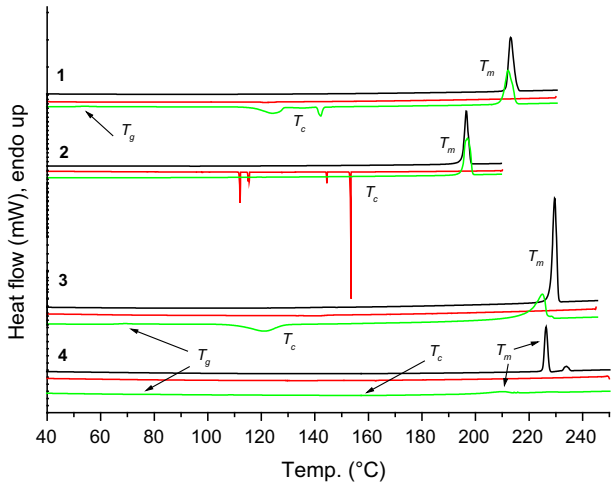

Fig. 7. DSC scans of **1**–**4**. For each compound: top = 1st heating; middle = cooling, and bottom scan = 2nd heating. T_m = melting, T_c = crystallization, T_g = glass transition.

and 8. The corresponding DSC and TG/DTA curves are illustrated in Figs. 7 and 8. The first DSC heating scans of **1**–**4** show single sharp melting endotherms at onset temperature of 211.5, 195.2, 227.9 and 225.2 °C, respectively. In addition, on **4** also an additional sequence of weak exo- and endothermic transitions are visible consecutively after the melting endotherm. These transitions appears to be originating as a result of partial re-crystallization of melt to a short-lived high temperature structure form that melts at 232.5 °C (ΔH = 5.55 kJ·mol^{-1}). On ensuing cooling scan, compounds **1**, **3** and **4** vitrify, and when heated for a second time a glass transition occurs first at 49.7, 64.3 and 75.1 °C, respectively, followed by a re-crystallization from 100 to 140 °C on **1** and **3**, and from 130 to 170 °C on **4**. Subsequently above crystallization the melting of original structure form is observed on **1** (see Supplementary material Table S1 for T_ms of 2nd heating scans), whereas weak melting endotherm appeared at 219.6 and 199.6 °C for **3** and **4**, respectively, thus indicating melting of a polymorphic form instead of the original one. Compound **2** exhibit sharp crystallization exotherm already on cooling (153.5 °C; ΔH = −31.52 kJ·mol^{-1}) and on a second heating scan, sharp melting transition of the original structure form is observed.

Inspection of thermodynamical characteristics reveals that sulfanilamide derivatives **1** and **2** have rather analogous T_ms with closely matching ΔH^T_{fus} and ΔS^T_{fus} values even though they are chemically different and hold clearly different HB geometries. Same trend, but with higher values, is observed also for benzamide derivatives **3** and **4** (Table 7). The amidation of sulfanilamide and the change of phenyl (**3**) to chlorophenyl group (**4**) appear to induce only minor change to the observed thermodynamic values. Based on the literature similar enthalpies of fusion and melting points have been reported to several sulfonamide derivatives, of which few are gathered to Table 7 for a comparison.

Thermal decomposition of compounds was examined with simultaneous TG/DTA analyzer. The resulted curves and thermal parameters are shown in Fig. 8 and Table 8, respectively. In all four cases three main degradation steps analogously to number of sulfonamides reported in the literature [54,55] can be observed. The first step indicative to thermal decomposition begins slowly at 240 °C(∼20–40 °C above T_m) accelerating gradually from decomposition onsets temperatures (T_d = 261, 257 261 and 271 °C for **1**–**4**, respectively). Thermal decomposition continues in the second step (temperature onsets about at 310–320 °C) with a higher weight

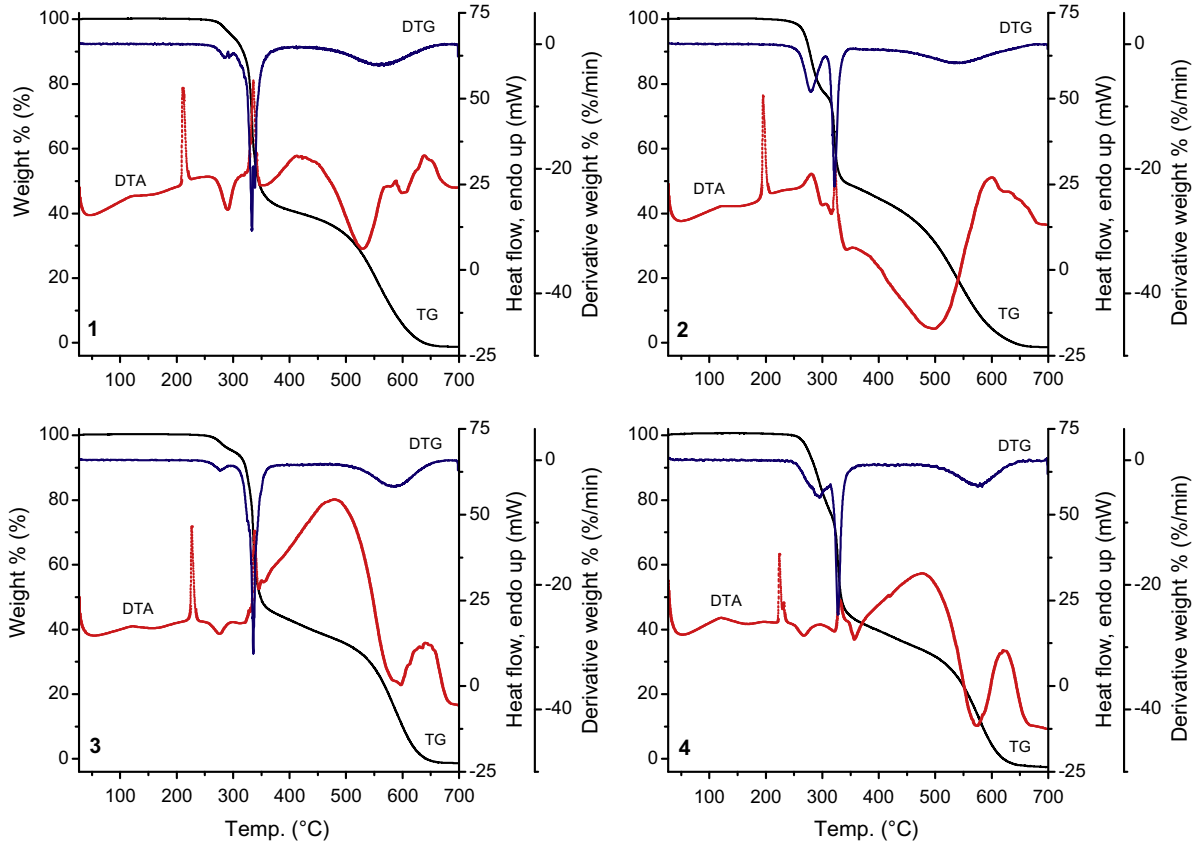

Fig. 8. TG, DTG and DTA curves of **1**–**4**.

Table 9
Zone inhibition values (in mm) of compounds with two concentrations (mg/ml).

Comp.	*S. Aureus*		*E. Coli*		*A. Niger*	*C. Albicans*
	10	100	10	100	10	10
1	17	26				
2	21	24		23		
Ciprofloxacin	40	40	40	40		
Miconazole					11	11

loss rate, that gradually slows down when proceeding to the third and final weight loss step (ranging from about 350–650 °C). Generally above 650 °C TG curves settle to near zero values (~1%) indicating nearly ashless residue. On **1** and **3** the first weight loss step is better resolved and clearly smaller in contrast to **2** and **4** in which the reactions of consecutive steps are significantly more overlapped. By combining first two steps, rather similar overall weight losses (~51–59%) can be obtained for all compounds. It is obvious that major degradation occurs on these steps but with slightly different kinetics and variation of reaction paths per substance. The third step is caused by further carbonization processes and slow combustion of the resulted molecular fragments. The decomposition products cannot be explicitly identified per step but it can be expected that various components like H_2O, NH_3, aromatic fragments (some halogenated on **4**), SO_2 and/or amines may be formed on the first two steps while CO and CO_2 are the main products of the last step. It is noticeable that the first weight loss step on amidated compounds **1**, **3** and **4** is exothermic (see DTA signals). Exothermic processes were also observed by Khattab et al. on decomposition of sulfonamides, such as sulfapyridine, sulfadiazine, sulfanilamide, sulfaphenazole and sulfathiazole [54]. As the range of functional groups in above molecules varies, it is assumed that the exothermic decomposition reactions may originate from a sulfamoyl core unit. This is further supported by the only amide-free compound **2** that at first show endothermic peak on first weight loss step but which turns exothermic in latter part of the step, thus the potential exothermic deamination on **1**, **3**, and **4** cannot be the only reason. Second step is uniformly endothermic (DTA peak maximum around at 330 °C) on all four compounds due the energy consuming fragmentation reactions occurring at the shown temperature range (Table and Fig. 8). Similarly the first part of the third step is endothermic due the carbonization but while the combustion processes gradually increase the DTA signal changes to exothermic.

3.6. Antimicrobial activity

The inhibition zones of the compounds are listed in Table 9. Compounds **1** and **2** have shown significant zone of inhibition for gram positive bacteria. But compounds **3** and **4** did not show any activity. No sample has shown antibacterial activity against gram negative bacteria except compound 1. The results indicate that there is no significant antibacterial activity with the introduction of the benzene ring to CO—NH group or SO_2—NH moiety. None of the samples have shown antifungal activity.

4. Conclusions

The present study reports the synthesis of four *N*-substituted sulfanilamide derivatives and their characterization, by analytical and physiochemical techniques. UV–Vis, NMR, FTIR and mass spectra of the derivatives have been recorded and interpreted. Thermal analysis and single crystal X-ray diffraction studies have also been performed. Single crystal diffraction analysis revealed compounds **1** and **2** to be crystallographically and conformationally (tilted V-shape) consistent crystallizing in orthorhombic *Pbca* space group. The benzamide containing sulfonamides **3** and **4** show L-shaped molecular conformation crystallizing in monoclinic $P2_1/c$ and triclinic *P*-1 space groups, respectively. The molecular conformations determined in this study can also be found in number of previously reported sulfonamides, of which the tilted V-shape appears to be somewhat more common one among the surveyed structures. On **1**, only ···H—N—C—O··· and ···H—N—S—O··· mediated hydrogen bond (HB) geometries with graph set notation of C(4) can be observed. These HBs form parallel HB chains running along *b*-axis. Also larger $R_4^4(26)$ type HB rings are formed as a combination of the simple basic C(4) HB units. The benzamidated derivatives **3** and **4** manifest L-shaped molecular conformation and have analogously C(8) type HB units that forms second level HB rings of $R_2^2(20)$ and $R_4^4(16)$ types. The only amide – free sulfanilamide derivative **2** exhibits C(8) HB basic units but in contrast to **3** and **4** different HB network of $R_4^4(22)$ and $R_2^2(6)$ type geometries are formed. Many of the observed HB geometries, such as C(8), $C_2^2(6)$ and $R_4^4(22)$ are also manifested frequently in other sulfonamides reported in the literature. Thermal characteristics of the examined compounds varied slightly in relation to the range of the substituents used. The melting points increased in order of **2** < **1** < **4** < **3** (195.2, 211.5, 225.2 and 227.9 °C, respectively), whereas **1** and **2** had enthalpies of fusion in the same order of magnitude (~37–38 kJ·mol^{-1}), as in the case of **3** and **4** albeit with somewhat higher enthalpies (~45–46 kJ·mol^{-1}). Thermal decomposition onset temperatures increased in order of **2** < **3** = **4** < **1** (257, 261, 261, 271 °C, respectively), thus the amide – free derivative **2** being the least and the acetamidated being the most thermally stable compound under the conditions used. Finally the antibacterial studies suggested that the introduction of the benzene ring to CO—NH group or SO_2—NH moiety hinders the significant antimicrobial activity.

Appendix A. Supplementary material

IR, NMR spectra, additional structure model figures and figure for the statistical distributions of various (dihedral) angles are included in the supplementary material. Crystallographic data for the compounds **1**–**4** have been deposited at the Cambridge Crystallographic Data Centre with the deposition numbers CCDC 947892-947895. Copies of the data can be obtained free of charge via external link http://ccdc.cam.ac.uk/retrieving.html. Supplementary data associated with this article can be found, in the online version, at http://dx.doi.org/10.1016/j.molstruc.2013.12.063.

References

[1] E.K. Kremer, G. Facchin, E. Estevez, P. Albores, E.J. Baran, J. Ellena, M.H. Torre, J. Inorg. Biochem. 100 (2006) 1167.
[2] M.E. Wolff, fifth ed., Burgers Medicinal Chemistry and Drug Discovery, vol. 2, Wiley, Laguna Beach, 1996. p. 528.
[3] J.R. Sorenson, J. Chem. Br. 1 (1984) 1110.
[4] E.J.E.F. Reynolds Martindale, The Extra Pharmacopoeia, 31st ed., Royal Pharmaceutical Society, London, 1996.
[5] A. Bult, Metal Ions in Biological Systems, Marcel Dekker, New York, 1983. p. 261.
[6] J. Drews, Science 287 (2000) 1960.
[7] M.A. Bhat, M. Imran, S.A. Khan, N. Siddiqui, Indian J. Pharm. Sci. 67 (2005) 151.
[8] M. Krátký, J. Vinsová, M. Volková, V. Buchta, F. Trejtnar, J. Stolaríková, Eur. J. Med. Chem. 50 (2012) 433.
[9] B.S. Priya, S.N. Swamy, M.V. Tejesvi, Basappa, G. Sarala, S.L. Gaonkar, S. Naveen, J.S. Prasad, K.S. Rangappa, Eur. J. Med. Chem. 41 (2006) 1262.
[10] C.T. Supuran, A. Innocenti, A. Mastrolorenzo, A. Scozzafava, Mini Rev. Med. Chem. 4 (2004) 189.
[11] Z. Huang, Z. Lin, J. Huang, Eur. J. Med. Chem. 36 (2001) 863.
[12] J.N. Domínguez, C. León, J. Rodrigues, N.G. de Domíngue, Jiri Gut, Philip J. Rosenthal, Il Farmaco 60 (2005) 307.
[13] A. Husain, Acta Pol. Pharm. Drug Res. 66 (2009) 513.
[14] C. Chazalette, B. Masereel, S. Rolin, A. Thiry, A. Scozzafava, A. Innocentic, C.T. Supuran, Bioorg. Med. Chem. Lett. 14 (2004) 5781.

[15] N. Siddiqui, N. Surendra Pandeya, A.S. Khan, J. Stables, A. Rana, M. Alam, M.F. Arshad, A.M. Bhat, Bioorg. Med. Chem. Lett. 17 (2007) 255.
[16] P. Alexiou, V.J. Demopoulos, J. Med. Chem. 53 (2010) 7756.
[17] L.R. Mcdougald, R.B. Galloway, Exp. Parasitol. 34 (1973) 39.
[18] A.E. Boyd, third ed. Diabetes 37 (1988) 847e850.
[19] C.T. Supuran, A. Scozzafava, Exp. Opin. Ther. Pat. 10 (2000) 575e600.
[20] T.H. Maren, Annu. Rev. Pharmacol. Toxicol. 16 (1976) 309e327.
[21] C.T. Supuran, A. Scozzafava, Curr. Med. Chem. Immunol. Endocr. Metabol. Agents 1 (2001) 61e97.
[22] C.W. Thornber, Chem. Soc. Rev. 8 (1979) 563e580.
[23] C.V.C. Prasad, W. Jeffery Noonan, P. Charles Sloan, W. Lau, S. Vig, F. Michael Parker, W. David Smith, B. Steven Hansel, Craig T. Polson, Dona M. Barten, M. Kevin Felsenstein, Susan B. Roberts, Bioorg. Med. Chem. Lett. 14 (2004) 1917.
[24] E.H. Northey, Chem. Rev. 27 (1940) 85.
[25] J.K. Seidel, J. Pharm. Sci. 57 (1968) 9.
[26] Collect, Bruker AXS Inc., Madison, 2008.
[27] Z. Otwinowski, D. Borek, W. Majewski, W. Minor, Acta Cryst. 59A (2003) 228.
[28] G.M. Sheldrick, SADABS. Version 2.3, Multi-Scan Absorption Correction Program, University of Göttingen, Germany, 2001.
[29] Agilent CrysalisPro, Agilent Technologies Ltd., Yarnton, England, 2010.
[30] G.M. Sheldrick, Acta Cryst. 64A (2008) 112.
[31] O.V. Dolomanov, L.J. Bourhis, R.J. Gildea, J.A.K. Howard, H. Puschmann, OLEX2: J. Appl. Cryst. 42 (2009) 339.
[32] C.J. Brown, D.S. Cook, L. Sengier, Acta Cryst. 40C (1984) 844.
[33] C.F. Macrae, I.J. Bruno, J.A. Chisholm, P.R. Edgington, P. McCabe, E. Pidcock, L. Rodriguez-Monge, R. Taylor, J. van de Streek, P.A. Wood, Mercury CSD 2.0 – New J. Appl. Cryst. 41 (2008) 466.
[34] R.J. Cremlyn, Chlorosulfonic Acid: A Versatile Reagent, The Royal Society of Chemistry, Cambridge, 2002.
[35] X. Deng, N.S. Mani, Green Chem. 8 (2006) 835.
[36] B.S. Furnis, A.J. Hannaford, P.W.G. Smith, A.R. Tatchell, Vogel's Textbook of Practical Organic Chemistry, fifth ed., Longman, London, 2002.
[37] B.T. Gowda, K. Jyothi, J. D'Souza, Z. Naturforsch. 57a (2002) 967.
[38] F.H. Allen, Acta Cryst. 58B (2002) 380.
[39] (a) G.L. Perlovich, A.M. Ryzhakov, V.V. Tkachev, L.K. Hansen, Cryst. Growth Des. 11 (2011) 1067;
(b) G.L. Perlovich, A.M. Ryzhakov, V.V. Tkachev, L.Kr. Hansen, O.A. Raevsky, Cryst. Growth Des. 13 (2013) 4002;
(c) G.L. Perlovich, N.N. Strakhova, V.P. Kazachenko, T.V. Volkova, V.V. Tkachev, K.J. Schaper, O.A. Raevsky, Int. J. Pharm. 334 (2007) 115;
(d) G.L. Perlovich, N.N. Strakhova, V.P. Kazachenko, T.V. Volkova, V.V. Tkachev, K.J. Schaper, O.A. Raevsky, J. Int. Pharm. 349 (2008) 300.
[40] A. Parkin, A. Collins, C.J. Gilmore, C.C. Wilson, Acta Cryst. 64B (2008) 66.
[41] E. Shefter, Cryst. Struct. Commun. 5 (1976) 847.
[42] G.L. Perlovich, V.V. Tkachev, N.N. Strakhova, V.P. Kazachenko, T.V. Volkova, O.V. Surov, K.J. Schaper, O.A. Raevsky, J. Pharm. Sci. 98 (2009) 4738.
[43] C.J. Kelly, J.M.S. Skakle, J.L. Wardell, S.M.S.V. Wardell, J.N. Low, C. Glidewell, Acta Cryst. 58B (2002) 94.
[44] P. John, I.U. Khan, M.A. Sajjad, S. Sharif, E.R.T. Tiekink, Acta Cryst. 66E (2010) o2031.
[45] S.M. Mirza, G. Mustafa, I.U. Khan, M. Zia-ur-Rehman, M. Shafiq, Acta Cryst. 67E (2011) o25.
[46] M. Ghosh, A.K. Basak, S.K. Mazumdar, B. Sheldrick, J. Cryst. Spectro. Res. 19 (1989) 289.
[47] M. Lahtinen, J. Damodara, P. Upadhyaya, Nonappa, E. Kolehmainen, Acta Cryst. 67E (2011) o2866.
[48] L. Li, F.Y. Meng, L. Wang, Z.F. Huang, S.Q. Wei, C.W. Lin, Z. Kristallogr. 227 (2012) 131.
[49] W.G. Pan, Z.D. Zhao, P. Luo, C.W. Lin, J.H. Miao, Acta Cryst. 68E (2012) o379.
[50] S. Yasmeen, S. Murtaza, M. Akkurt, I.U. Khan, S. Sharif, Acta Cryst. 66E (2010) o2264.
[51] M.C. Etter, Acc. Chem. Res. 61 (1990) 120.
[52] Assignments for the moieties formed via intermolecular HBs described by Etter [51] are as follows: C (chain) and R (ring). The number of proton donors (d) and acceptors (a) used in each moiety are assigned as subscripts and superscripts, respectively, and the size or degree of the moiety (corresponding to the number of atoms in the repeating unit) is indicated in parentheses.
[53] S.S. Yang, J.K. Guillory, J. Pharm. Sci. 61 (1972) 26.
[54] M. Wesołowski, E. Kosecka, J. Erecińska, K. Kobyłczyk, J. Therm. Anal. Calorim. 74 (2003) 465.
[55] L.E. Cook, D.A. Hildebrand, Thermochim. Acta 9 (1974) 129.